Neutron scattering and electrical transport in $Nd_{0.5}Pb_{0.5}MnO_3$

1989 J. Phys.: Condens. Matter 1 2721

(http://iopscience.iop.org/0953-8984/1/16/009)

J. Phys.: Condens. Matter 1 (1989) 2721–2726. Printed in the UK

LETTER TO THE EDITOR

Neutron scattering and electrical transport in $Nd_{0.5}Pb_{0.5}MnO_3$

K N Clausen†, W Hayes‡, D A Keen‡, R M Kusters§, R L McGreevy‡ and J Singleton§

† Risø National Laboratory, Postbox 49, DK-4000 Roskilde, Denmark

‡ Clarendon Laboratory, Parks Road, Oxford OX1 3PU, UK

§ High Field Magnet Laboratory and Research Institute for Materials, University of Nijmegen, Toernooiveld 1, 6525ED Nijmegen, The Netherlands

Received 30 November 1988, in final form 2 February 1989

Abstract. Diffuse neutron scattering measurements have been made on single crystals of $Nd_{0.5}Pb_{0.5}MnO_3$ in the temperature range 5–295 K. It is found that $Nd_{0.5}Pb_{0.5}MnO_3$ begins to order magnetically at a temperature $T_c \simeq 184$ K, this being accompanied by an anomalous change in electrical conductivity. Above T_c the conductivity is of the activated hopping type and below T_c it is metallic. Neutron scattering measurements show that below T_c there are well defined magnon branches which soften as T approaches T_c. Temperature-dependent coherent diffuse quasi-elastic scattering occurs around some Bragg peaks above T_c. This diffuse scattering is magnetic in origin and its energy width is consistent with the activation energy derived from the conductivity, suggesting magnetic polaron formation. Diffuse scattering due to lattice polarons has not been observed.

Diffuse quasi-elastic neutron scattering can be used to study the structure and dynamics of point defects in crystals. Coherent diffuse neutron scattering originates from local deviations from the long-range order, i.e. neutrons scatter from the distortions of the lattice or magnetic spin density associated with defects. Thermally induced ionic defects in fluorite crystals have been the subject of detailed study by this method (see, for example, Hutchings *et al* (1984) and Andersen *et al* (1987)). It has been suggested by Gillan and Wolf (1985) that the technique may also, in principle, be applied to a study of ionic polarons. In non-magnetic polaronic materials electronic conduction is caused by activated hopping of the carrier together with the lattice distortion associated with it. In magnetic materials the formation of magnetic polarons, in which the carrier spin-polarises the magnetic ions around it, is also possible (Shapira *et al* 1974).

We have used the technique of diffuse neutron scattering to investigate polarons in $Nd_{0.5}Pb_{0.5}MnO_3$. Neutron experiments were carried out on a variety of triple-axis spectrometers: IN12 on the cold source at the Institut Laue–Langevin for high-resolution inelastic measurements, TAS6 at Risø National Laboratory for elastic diffuse scattering measurements, and TAS7 at Risø using cold-polarised neutrons for polarisation analysis. $Nd_{0.5}Pb_{0.5}MnO_3$ was chosen for these initial investigations as good single crystals ($\simeq 0.5$ cm^3) were available, grown by a flux technique (Morrish *et al* 1969). Transport studies of a similar material, $La(Sr)CrO_3$, have shown electrical conductivity due to hopping of localised lattice polarons (Karim and Aldred 1979). In $Nd_{0.5}Pb_{0.5}MnO_3$, Pb^{2+}

0953-8984/89/162721 + 06 $02.50

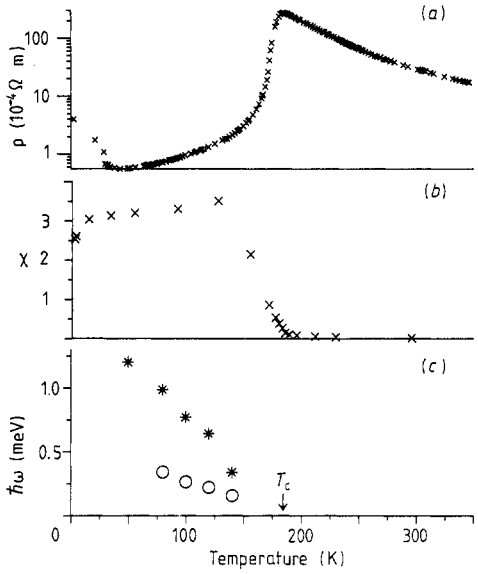

Figure 1. Effects of the magnetic transition in $Nd_{0.5}Pb_{0.5}MnO_3$. (*a*) Four-contact AC resistivity as a function of temperature with current in the [100] direction. (*b*) Temperature dependence of the AC magnetic susceptibility (powder sample). (*c*) Temperature dependence of magnon energies around the (100) Bragg peak: ○, $q = (0.95, 0, 0)$; *, $q = (0.9, 0, 0)$.

from the lead oxide flux dissolves in Nd^{3+} sites, leading to a mixed Mn^{3+}/Mn^{4+} valence; this mixed valence gives rise to conduction, as in $La_2(Sr)CuO_4$ (Bednorz and Müller 1986). Pure $NdMnO_3$ has an orthorhombically distorted perovskite structure (Quezel-Ambrunaz 1968); however, in our mixed crystals the distortion has almost totally disappeared such that $Nd_{0.5}Pb_{0.5}MnO_3$ may be considered to be cubic (but see later). Further details of both the lattice and magnetic structure, obtained by powder and single-crystal neutron diffraction measurements, will be reported in a later paper (Clausen *et al* 1989).

The samples were initially characterised by electron probe microanalysis to establish the $Nd^{3+}:Pb^{2+}$ ratio, which was found to be 1:1. Subsequently six silver contacts, in a 'Hall bar' configuration, were evaporated onto $10 \times 2 \times 2\ mm^3$ blocks cut from single crystals, with their long axes along the [100] or [110] directions, in order to allow resistivity measurements to be made. Typical data are shown in figure 1(*a*). A maximum in resistivity occurs at $T_c = 184 \pm 1$ K and above this temperature the transport is activated, with an activation energy of 95 ± 5 meV.

Magnetoresistance measurements at fields of up to 20 T have shown that the conductivity above T_c is due to hopping of localised magnetic polarons, which have a mobility of $\approx 0.1\ cm^2\ V^{-1}\ s^{-1}$ (Kusters *et al* 1989). Below T_c the resistivity falls rapidly, and then approximates to metallic behaviour. However, at the very lowest temperatures the resistivity increases again (see below), and this effect is at present under detailed investigation. Measurements made with the current along [100] and [110] crystal directions showed no anisotropy in the resistivity.

Static magnetisation measurements were also made on the same samples and on $Nd_{0.5}Pb_{0.5}MnO_3$ powder using a Foner magnetometer. Figure 1(*b*) shows typical susceptibility data for a powder sample. It can be seen that the peak in resistivity coincides with the onset of ferromagnetic order. In our mixed crystal, transition to an ordered state is not abrupt and full analysis shows that complete order occurs at around 145 K (Kusters *et al* 1989). Measurements of the neutron Bragg scattering as a function of

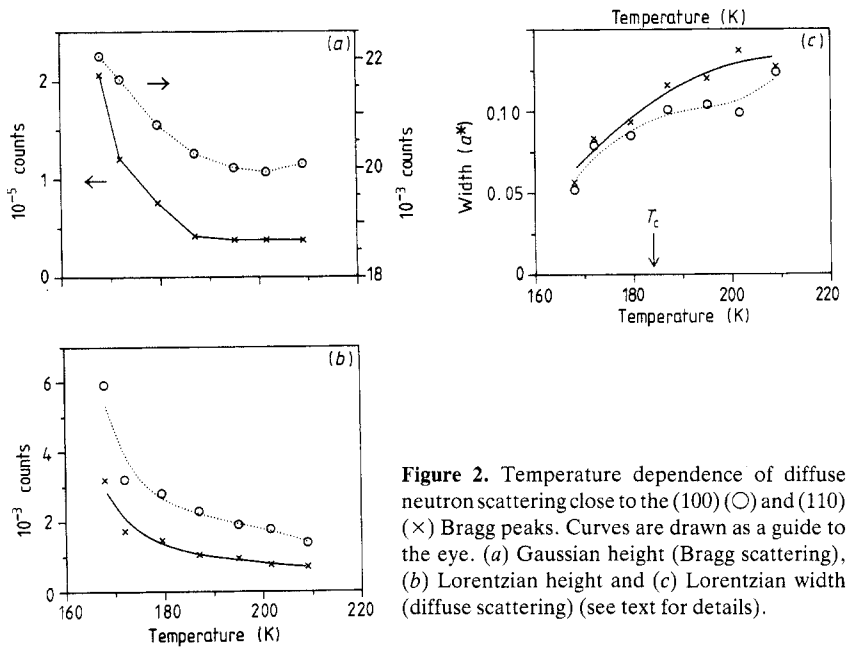

Figure 2. Temperature dependence of diffuse neutron scattering close to the (100) (○) and (110) (×) Bragg peaks. Curves are drawn as a guide to the eye. (*a*) Gaussian height (Bragg scattering), (*b*) Lorentzian height and (*c*) Lorentzian width (diffuse scattering) (see text for details).

temperature show that the transition corresponds to ferromagnetic order in the Mn sublattice (Clausen *et al* 1989). This is in contrast to 'pure' $NdMnO_3$, where antiferromagnetic order was seen with a Néel temperature ranging from 85–112 K (Pauthenet and Veyret 1970, Vickery and Klann 1957); possible reasons for this variation have been discussed elsewhere (Kusters *et al* 1989). The Nd moments order below 30 K, canted with respect to the Mn moments, and it remains to be established whether this ordering has any connection with the increase in resistivity seen below that temperature (figure 1(*a*)).

Elastic diffuse scattering measurements were made on two crystals of $Nd_{0.5}Pb_{0.5}MnO_3$ and the results are in good agreement. Temperature-dependent coherent diffuse scattering was observed both close to and away from Bragg peaks. In figure 2 the height and width of the diffuse contribution close to (100) and (110) peaks are shown, together with the height of the Bragg contribution. The data have been obtained by fitting a resolution-width Gaussian (Bragg contribution) and a variable-width Lorentzian (diffuse contribution) to ω–2θ scans across the Bragg peaks. In the case of elastic Bragg scattering (figure 2(*a*)) there is a well defined change of intensity at T_c, whereas there is no obvious change in elastic diffuse scattering (figures 2(*b*) and 2(*c*)). Figure 3 shows contour plots of scattering in the (001) plane, with contours chosen to display the weak scattering in the vicinity of Bragg peaks. Small Bragg peaks occur at half-points (e.g. $(\frac{1}{2}00)$, $(\frac{1}{2}\frac{1}{2}0)$) due to a doubling of the (cubic) unit cell by the slight residual distortion; these are three orders of magnitude weaker than other Bragg peaks. Diffuse scattering close to (100) and (110) peaks is strongly temperature dependent; further away the scattering centred around (110) has a complex temperature variation, while that around (100) is almost temperature independent.

The magnetic transition is clear in the inelastic diffuse scattering (figure 1(*c*)). Below 140 K magnon branches are observed which soften as temperature is increased and the magnon energy extrapolates to zero at 180 ± 5 K. Above this temperature the scattering becomes quasi-elastic, corresponding to a change from long-range to short-range mag-

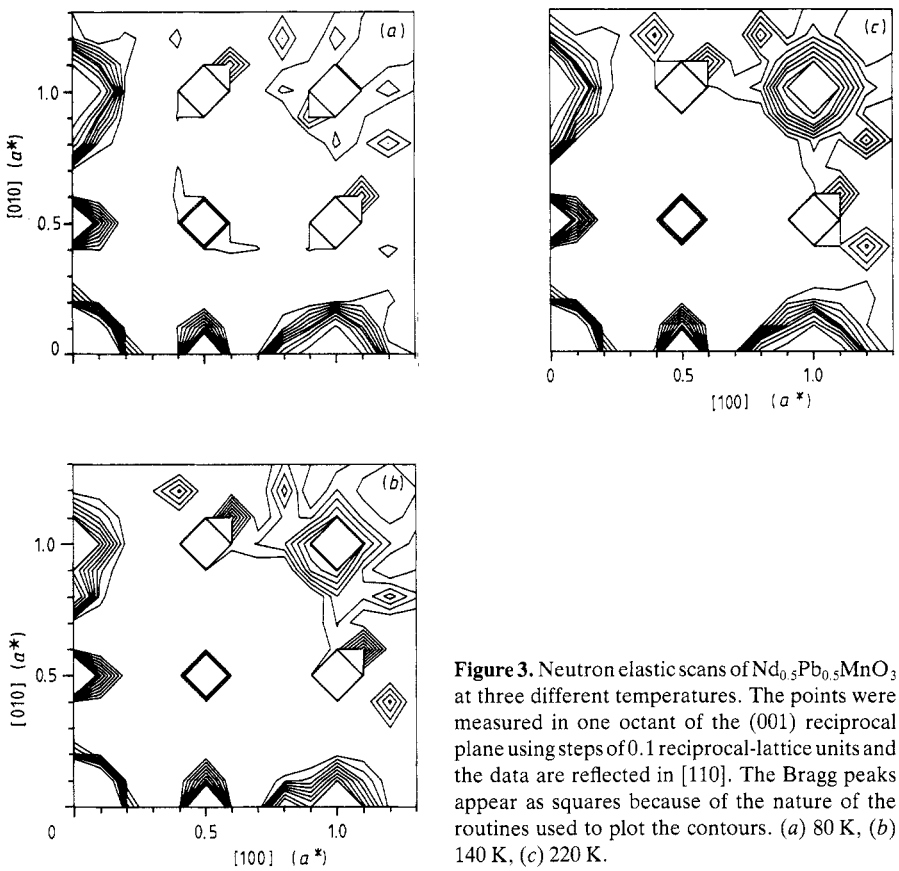

Figure 3. Neutron elastic scans of $Nd_{0.5}Pb_{0.5}MnO_3$ at three different temperatures. The points were measured in one octant of the (001) reciprocal plane using steps of 0.1 reciprocal-lattice units and the data are reflected in [110]. The Bragg peaks appear as squares because of the nature of the routines used to plot the contours. (*a*) 80 K, (*b*) 140 K, (*c*) 220 K.

netic order. The energy width observed as a function of temperature gives an activation energy of 80 ± 20 meV and a mobility of $\simeq 0.1\ \mathrm{cm^2\ V^{-1}\ s^{-1}}$, consistent with values derived from the transport measurements (Kusters *et al* 1989). The diffuse contribution to the $\int S(Q, \omega)\, \mathrm{d}\omega$ increases with temperature, as more polaronic carriers become thermally activated. This is opposite to the expected behaviour for diffuse magnetic critical scattering.

Polarisation analysis provides a method for determining the cause of the diffuse scattering observed above T_c. Using incident neutrons polarised parallel to the scattering vector and analysing the polarity of the scattered beam, magnetic and coherent nuclear scattering can easily be separated. All magnetic scattering is spin-flip scattering whereas nuclear coherent and isotopic incoherent scattering is non-spin-flip (Moon *et al* 1968). Polarisation analysis was only employed above T_c, since depolarisation of the neutron beam was observed below T_c, as expected for a multidomain ferromagnet. Figure 4 shows an ω–2θ elastic scan through the (110) peak at $T = 208$ K. The fact that diffuse scattering is observed for spin-flip but not for non-spin-flip scattering means that the diffuse scattering is magnetic. Around this peak the nuclear contribution to the diffuse scattering is too small to distinguish within the errors. However, close to the non-magnetic Bragg peak $(1\frac{1}{2}\ \frac{1}{2}\ 0)$ a weak coherent nuclear contribution is observed.

In conclusion, we have shown that the measured diffuse scattering can be identified with magnetic polaron hopping above T_c. The magnetic polarisation caused by the

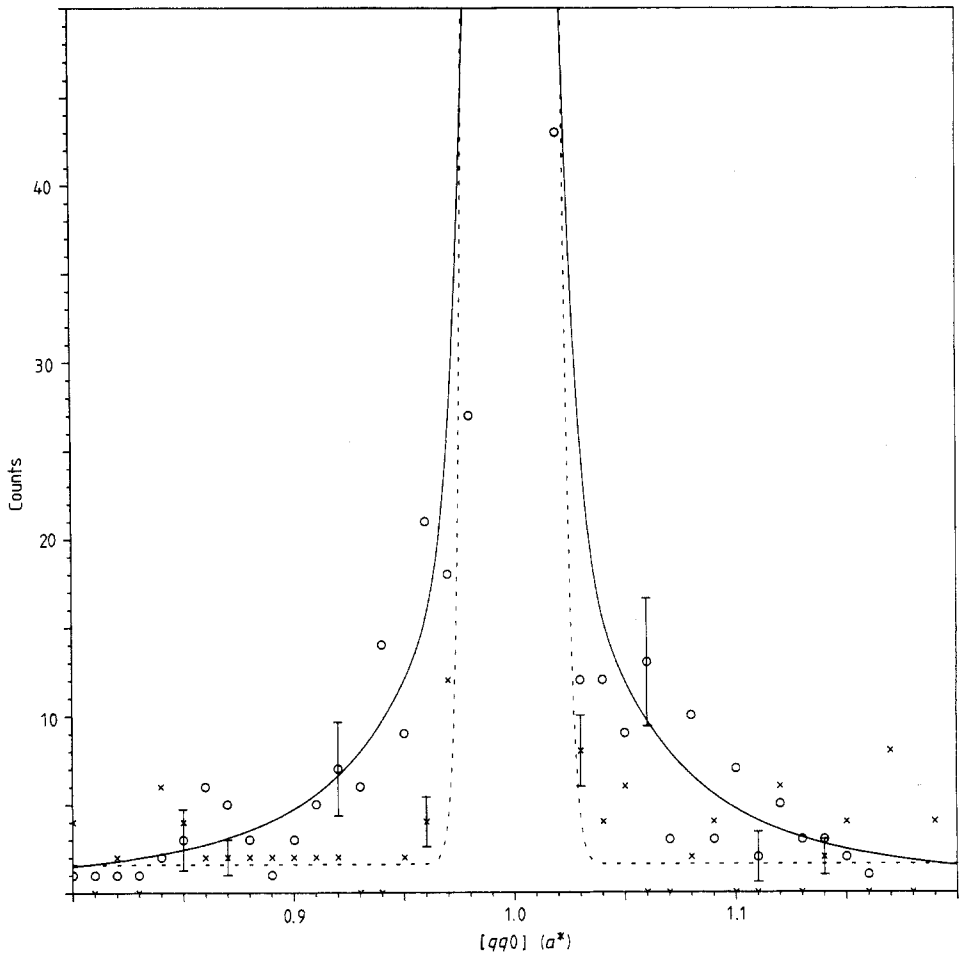

Figure 4. ω–2θ scan across the (110) Bragg peak at 208 K using polarised neutrons. Circles and full curve, spin-flip scatter; crosses and broken curve, non-spin-flip scatter. Curves are drawn as a guide to the eye.

carriers decreases as magnetic order increases and below T_c carrier localisation becomes negligible; this corresponds to the rapid fall in resistivity. The mobility and activation energy derived by neutron scattering and transport measurements are in good agreement. Diffuse scattering due to lattice polarons has not been observed because of the strong diffuse magnetic scattering. Future studies on a non-magnetic polaronic conductor should provide a clearer indication of the possible usefulness of diffuse neutron scattering as a technique for investigating lattice polarons.

We are grateful for the technical assistance of F Wittekamp and J A A J Perenboom at the High Field Magnet Laboratory, University of Nijmegen, to L Cussens at the Institut Laue–Langevin and to the Hahn–Meitner Institut in Berlin for the use of their super-mirror polarisers. Two of us (DAK and RLM) thank Risø National Laboratory for their hospitality. This work was supported by the SERC (UK), the FOM and NWO (Netherlands) and Nato Collaborative Research Grant 0141/88.

References

Anderson N H, Clausen K N and Kjems J K 1987 *Methods of Experimental Physics* vol 23, part B, ed. D L Price and K Skold (New York: Academic) p 187
Bednorz J G and Müller K A 1986 *Z. Phys.* B **64** 189
Clausen K N *et al* 1989 to be published
Gillan M J and Wolf D 1985 *Phys. Rev. Lett.* **55** 1299
Hutchings M T, Clausen K N, Dickens M H, Hayes W, Kjems J K, Schnabel P G and Smith C 1984 *J. Phys. C: Solid State Phys.* **17** 3903
Karim D P and Aldred A T 1979 *Phys. Rev.* B **20** 2255
Kusters R M, Singleton J, Keen D A, McGreevy R L and Hayes W 1989 *Physica* B+C submitted
Moon R M, Riste T and Koehler W C 1968 *Phys. Rev.* **181** 920
Morrish A H, Evans B J, Eaton J A and Leung L K 1969 *Can. J. Phys.* **47** 2691
Pauthenet R and Veyret C 1970 *J. Physique* **31** 65
Quezel-Ambrunaz S 1968 *Bull. Soc. Fr. Minéral. Crystallogr.* **91** 339
Shapira Y, Foner S, Oliveira N F and Reed T B 1974 *Phys. Rev.* B **10** 4765
Vickery R C and Klann A 1957 *J. Chem. Phys.* **27** 1161